Heterogeneous & Homogeneous & Bio- & Nano-
CHEMCATCHEM
CATALYSIS

Accepted Article

Title: Oxidative esterification of methacrolein to methyl methacrylate over supported gold catalysts prepared by colloid deposition

Authors: Yuchao Li, Yanxia Zheng, Lei Wang, and Zhongjun Fu

To be cited as: *ChemCatChem* 10.1002/cctc.201601688

Link to VoR: http://dx.doi.org/10.1002/cctc.201601688

A Journal of
ChemPubSoc Europe

WILEY-VCH

www.chemcatchem.org

ChemCatChem 10.1002/cctc.201601688

Oxidative esterification of methacrolein to methyl methacrylate over supported gold catalysts prepared by colloid deposition

Yuchao Li, *[a] Yanxia Zheng, [a] Lei Wang[b] and Zhongjun Fu[a]

Abstract: Esterification is one of the most pivotal organic transformations. Au catalysts were prepared by colloid deposition method using poly vinyl alcohol (PVA) as protective agent for the oxidative esterification of methacrylate (MAL) to methyl methacrylate (MMA). Three pre-treatments were used to remove the PVA, which is unfavorable for catalytic activity. It is found that the catalyst pre-treated at 300 ºC substantially improved activity due to the reduced PVA loading compared with hot water washing and water reflux. Surprisingly, it is also found that the distribution and loading content of Au particles was closely related to the pH of the colloid solution. We demonstrate that the deposition process is controlled by the different charge of the support surface at different colloid solution pH. Further, the catalysts with the similar size of Au particles loaded on TiO_2, SiO_2, Al_2O_3, CeO_2, ZrO_2 and ZnO were successfully prepared by controlling the colloid solution pH. The Au/ZnO presented the best performance, which may be due to the strong basic surface sites that improved the formation of the intermediate and the strong interaction between Au and ZnO. This interaction caused the anchoring effect and the change of geometries of Au particles which could enhance the stability of catalysts and promote the mobility of oxygen respectively.

Introduction

MMA is an important industrial material, which can be used to produce acrylic plastics and other polymer dispersions used in paints and coatings.[1] Currently, MMA is mainly produced by the acetone cyanohydrins process (ACH), but there are challenges to deal with the byproduct ammonium bisulfate waste and toxic raw material hydrogen cyanide. Hence, some environmentally friendly starting alternatives have been developed such as isobutene and syngas, which are firstly converted to MAL and then oxidative esterification to MMA. The oxidative esterification of MAL with methanol to MMA is the key step in these attractive routes for the production of MMA (Scheme 1).

Recently, Au based catalysts have been reported for the direct oxidative esterification of MAL efficiently due to their high activity in many reactions to replace the traditional Pd-Pb catalysts, which generally showed a selectivity for MMA below 90% and the Pb is quite toxic.[2] In addition, in most case, the alkali $Mg(OH)_2$ is required to obtain high yield of ester,[3] which makes the whole route less green and more expensive. Others employed MgO as promoter or support to prepare MMA with low conversion[4] or high content of methanol[5] which goes against the commercial applications due to the energy-extensive consumption for separation. Au nanoparticles supported on lots of metal oxides have been investigated on oxidative esterification of primary aldehyde or alcohol with alcohol to corresponding ester with a high activity. Although it is reported that the acidic sites[6] or basic sites[5] of support was in favor of the activity of catalysts, it is unknown that how the acidic sites or basic sites patticipate in the reaction process and whether there is other prior factor that affects the performance of catalysts. The intrinsic effect of the support still need to be investigated in order to further understand the roles of the support.

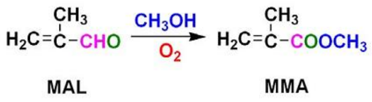

$$H_2C{=}\overset{CH_3}{C}{-}CHO \xrightarrow[O_2]{CH_3OH} H_2C{=}\overset{CH_3}{C}{-}COOCH_3$$

Scheme 1. Oxidative esterification of MAL with methanol to produce MMA

In addition, the Au particle size and designed morphologies also have an important effect on the activity of catalysts. Among the reported catalysts, the main preparation method is deposition-precipitation (DP) method, which is not fit for all support especially for support with low isoelectric point.[7] Moreover, it is hard to precisely control the loading content, the particle size and the morphologies of Au by DP method. In this paper, we focus on the colloid deposition method since it is possible to precisely tune the particle size distribution and morphology before deposition on the support. Thus, the effect of the intrinsic support could be easy to investigate. However, the polymer ligands or surfactants are typically required to stabilize the Au nanoparticles during the colloid deposition method. The stabilizing ligands associated with the Au particles as well as the support, which leads to the decrease of active sites. It is expected that those ligands will reduce the activity of catalysts. Hence, it is necessary to remove these stabilizing ligands, nevertheless, it is difficult to remove by only traditional washing. Recently, post-synthesis heat or extraction treatment methodologies have been developed for removing the stabilizing ligands after the immobilization step. For instance, it is found that using an appropriate calcination procedure these ligands could be effectively removed and the catalysts are active for CO oxidation without causing a significant increase in the mean particle size.[8] It is also reported that using hot water washing or hot water reflux could be efficient to remove the ligands and greatly improve the activity of catalysts.[9] And both found that the Au supported on TiO_2 presented the best performance. However, the effect of textural structure of support to the preparation process and the activity of catalyst was not discussed in detail. Ke et al. prepared the Au catalysts by the colloidal deposition method using PVA as protecting agent and

---

[a] Dr. Y. Li, Y. Zheng, prof. Z. Fu
School of Chemical Engineering
Shandong University of Technology
Zibo 255049, PR China
E-mail:cyulee@126.com
[b] Dr. L. Wang
State Key Laboratory of Multiphase Complex Systems
Institute of Process Engineering, Chinese Academy of Sciences
Beijing 100190, PR China

Supporting information for this article is given via a link at the end of the document.

investigated the effect of support on oxidative esterification of ethylene glycol.[10] But, the effect of PVA was not involved.

Recently, we have aimed at developing efficient Au catalysts using colloid deposition method applied for the oxidative esterification of MAL with methanol to MMA in the absence of any liquid bases. To obtain the best performance, we firstly examine the ways of removing PVA included the calcination and hot water pretreatment, as well the effects on the structure and activity of those catalysts. The effects of pH during the immobilization step were investigated. The effects of the support and the reason for the high activity of ZnO supported Au catalyst were discussed.

Results and Discussion

Effective PVA removing method to minimize its negative effect on the catalytic performance

The stabilizers are still associated with the Au particles as well as the support after the deposition, which could obviously affect the activity of catalysts. Therefore, it is necessary to remove the PVA ligands to activate the Au particles and support after the immobilization. However, one of the challenges is the loss of activity due to the sintering of the Au particles during the removal process. We investigated three methods to remove stabilizer PVA including the thermal treatment, hot water washing and hot water reflux. The evaluation of the size of Au particles supported on ZnO after different treatments was carried out by TEM technology and the representative micrographs and corresponding particle size distributions are shown in Fig. 1. The mean Au particle size of samples treated only dry at 100 °C or only washing by 90 °C hot water presented 4.16 nm or 4.09 nm. After the heat treatment at 300 °C for 4 hours or water reflux, the mean size of Au particles increased slightly to 4.4 nm. Thus, these three treatments did not affect the Au particle size distributions and they basically presented similar size around 4.2 nm, which is close to the Au colloid size (Figure 1f).

Further, the DT-TGA analysis was used to investigate the PVA content after treatments. The spectra of DT-TGA are shown in Figure 2 and the analysis data are presented in Table 1. For all of the samples, an obvious exothermic peak could be observed around 250 °C, which was assigned to the decomposition of PVA stabilizer. Besides, the dramatic weight loss from 100 °C to 300 °C could be also observed and the weight of catalysts mostly kept the same after 450 °C. These findings suggest that the PVA started to decompose around 100 °C and at 250 °C decomposed the most quickly, and finally, it could be totally removed above 450 °C. With the increase of treatment temperature from 100 °C to 450 °C, the weight loss (WL$_{100\text{-}450}$) of samples (Table 1) decreased from 0.38% to 0.14%. Hence, the heat treatment is an effective method to remove the PVA, although little PVA still stayed on the catalyst after calcination at 300 °C. The thermal treatment at 400 °C was not adopted due to the dramatic increase of Au particle size leading to the deactivation of catalyst. The WL$_{100\text{-}450}$ for the sample treated by hot water washing presented 0.33%, which is similar with the sample only dry at 100 °C. Hence, the hot water washing method is not an effective way to remove the PVA stabilizer. The water reflux is a better method than the hot water

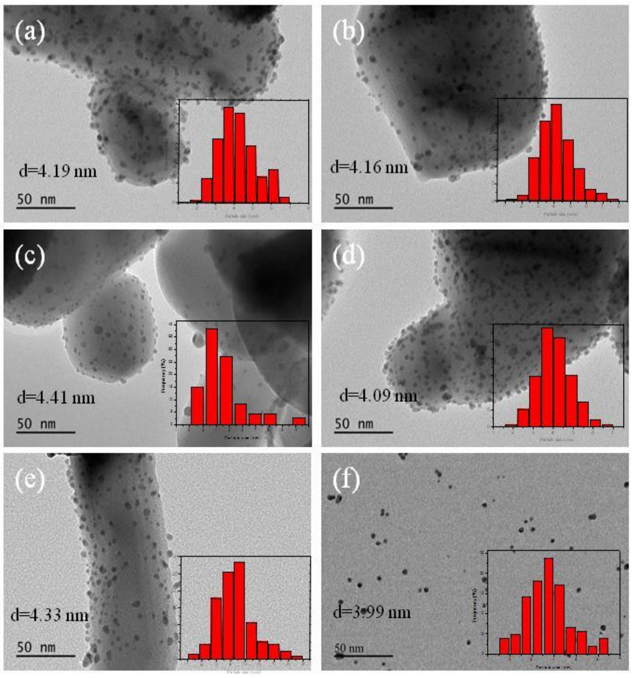

Figure 1. TEM micrographs of Au/ZnO catalysts after different methods of removing PVA and the corresponding particle size distributions data. (a) dry at 100 °C, (b) calcined at 200 °C, (c) calcined at 300 °C, (d) 90 °C water washing, (e) 90 °C water reflux for 2h, (f) gold colloid before deposition

Table 1. Catalytic performance of catalysts with different PVA removal methods[a] and corresponding catalysts weight loss and surface atomic ratio of Au

PVA removal method	WL$_{100\text{-}450}$ [%]	Surface atomic ratio of Au [%]	Conversion of MAL [%]	Selectivity (%)[b]		
				MMA	Acetal	Others
Calcination at 100 °C	0.38	6.6	56.4	46.5	4.1	8.2
Calcination at 200 °C	0.22	6.8	97.9	74.4	0.8	8.0
Calcination at 300 °C	0.14	7.3	99.9	85.9	0.6	7.63
Water reflux	0.28	6.7	90.5	70.9	3.7	5.3
Hot water washing	0.33	6.6	52.8	32.9	3.7	9.5

[a] Reaction conditions: catalyst (Au loading, 1 wt %), 0.50 g; CH_3OH/MAL = 30:1 (molar ratio); CH_3OH, 15 mL; P (O_2) = 0.2 MPa; T = 343 K; t = 2 h. [b] MMA, methyl methacrylate; others include methyl isobutyrate, isobutyric acid, isobutyl aldehyde, dimers of the methacrolein, and some unknown products.

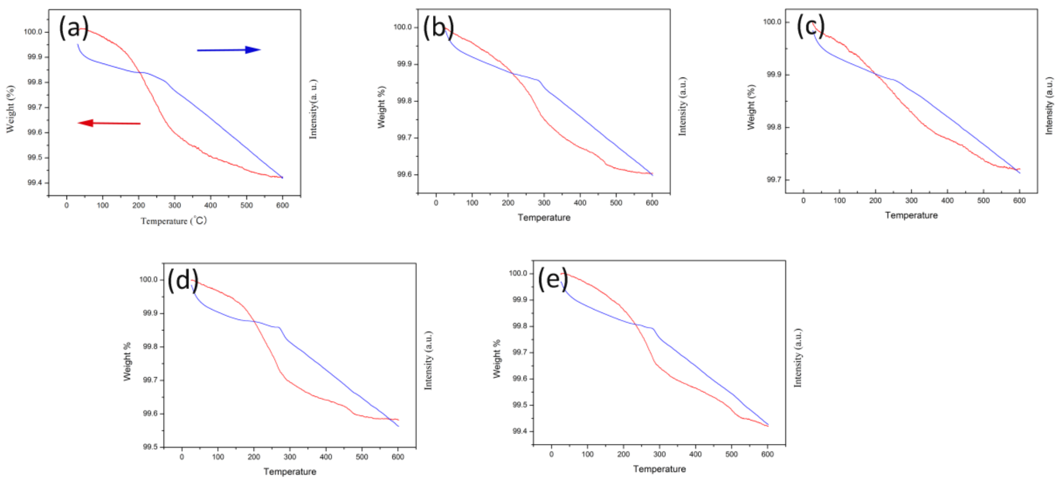

Figure 2. DT-TGA spretra of Au/ZnO catalysts after different methods of removing PVA. (a) dry at 100 ºC, (b) calcined at 200 ºC, (c) calcined at 300 ºC, (d) 90 ºC water washing, (e) 90 ºC water reflux for 2h.

washing due to that the $WL_{100\text{-}450}$ presented 0.28%. Comparatively, the hot treatment is the most efficient method.

XPS technology was employed to analyze the Au valence state and surface atomic ratio. The binding energy of Au (Figure S1) for catalysts with different PVA removal methods located the similar position, hence, indicating that treatments did not change the Au valence state. However, the surface atomic ratio of Au is different (Table 1). The sample calcined at 300 ºC possessed highest Au atomic ratio at 7.3%, while the others presented around 6.7%. This means that more Au sites exposed outside due to the efficient removal of PVA. The catalysts with different PVA removal methods were tested on the oxidative esterification of MAL to MMA and the results are shown in Table 1. The catalysts thermally treated at 100 ºC or treated by hot water washing presented bad activity with the conversion of MAL around 55% and selectivity of MMA around 40%. Many side reactions occurred and the main by-products included 1,1-dimethoxy-2-methylpropylene (acetal), Methyl isobutyrate (MIB), isobutyl aldehyde, dimers of the methacrolein, and CO_2, which are products of over-oxidation and generally produced more with the increased of conversion of MAL. The catalysts calcined at 200 ºC or treated by water reflux showed medium activity with conversion of MAL about 95% and selectivity of MMA about 70%. The catalyst calcined at 300 ºC provided the best catalytic performance with the conversion of MAL above 99% and the selectivity of MMA 85.9%. This activity of catalysts trends against with the content of PVA. Therefore, the content of PVA significantly affected the activity of Au particles and the thermal treatment is an effective way to remove the PVA. The method of pre-treatment by hot water washing could not be profitable to remove the PVA stabilizer, which may due to that the time of washing is too short to dissolve PVA by hot water. The water extraction method is a relative good way to remove PVA. Although the catalyst pre-treated by water reflux possessed more PVA than the sample calcined at 200 ºC, it presented similar catalytic activity. This relative enhancement of activity may be due to the smaller average Au particle size (4.09 nm) than the sample calcined at 200 ºC. Hence, the water reflux could remove PVA without Au particles increasing obviously. However, the catalyst after water reflux once as reported in literature could not be efficient to catalyze the oxidative esterification of MAL. To improve the removal of PVA, further measures should be carried out such as multi water reflux, which is under study in our group.

In summary, we compared catalysts with three different pre-treatment methods to remove the PVA stabilizer. The heat thermal treatment presented the best activity with the slight increase of mean Au particles size. The water reflux method could improve the catalytic performance without the growth of Au size. Besides, no matter which way was used to remove the PVA, the valence state of Au was metal state with binding energy around 83.7 eV assigned to the strong interaction between Au particles and ZnO support.

Effects of colloid solution pH on the size of supported Au particles

Traditionally, it is expected that the colloid deposition process should not alter the particle sizes and distributions, because the gold clusters had been produced before deposition. It is also reported that the Au nanoparticles would be completely adsorbed on supports after enough time.[8] However, we found that the supports with low isoelectric point could not completely adsorb the Au particles and the size of Au particles grew up. The distribution of Au nanoparticles and the loading content of Au were depended on the point of zero charge of the support during the immobilization step. To investigate this effect in detail, CeO_2 and ZrO_2 were selected due to their proper isoelectric point around 6.5, since the Au colloid solution pH was around 9 without adjustment

10.1002/cctc.201601688

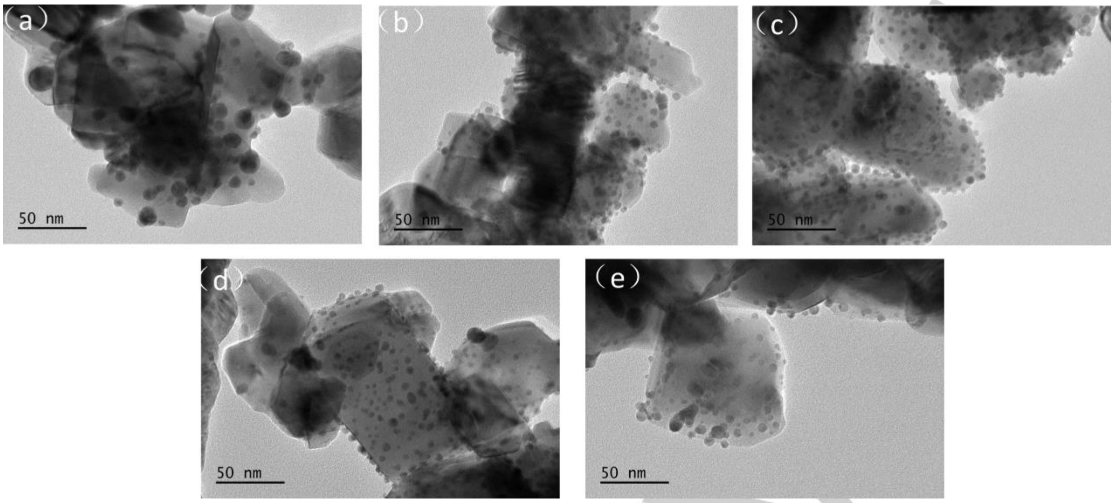

Figure 3. TEM micrographs of Au/CeO_2 catalysts prepared under different colloid solution pH and the corresponding particle size distributions. (a) pH=9, (b) pH=7, (c) pH=5, (d) pH=3, (e) pH=1

by HCl solution. Thus, it is not easy to show the relationship between the solution pH value and the isoelectric point of support due to the high isoelectric point of ZnO and Al_2O_3 around 10. The Au particles were adsorbed on CeO_2 with different colloid solution pH and the typical TEM micrographs are shown in Figure 3.When the pH value (pH=9) was above the isoelectric point, the Au particles became bigger during deposition from 4.3 nm to 5.1 nm (Table S1), while the mean size of Au particles was around 4.4 nm at the colloid solution pH in the range of 3-7. The size and distribution of Au particles did not alter during the deposition process, when the colloid solution pH was around the isoelectric point of support. However, the size of Au particles supported on CeO_2 increased to 8.1 nm with the pH value decreasing around 1. The similar trend could also been observed for the Au particles loaded on ZrO_2 with the change of pH value (Figure. S2). Thus, these results allow us to propose that the size of Au particles decreased at first then increased for other supports with the decrease of pH around the isoelectric point of corresponding support.

On the other hand, the surface area of support also affects the deposition process. The size of Au particles supported on ZrO_2 changed smaller from 4.5 nm to 5.5 nm than the samples supported on CeO_2 from 4.3 nm to 8.1 nm. Besides, the Au colloid could completely deposit (Table S1) on the ZrO_2 varying different pH, while part of Au particles still stayed in solution after deposition on CeO_2 at the pH 7-9 above the isoelectric point of CeO_2. This means that other factors of the support also play important role on the Au deposition process eliminating the solution pH and the isoelectric point. The ZrO_2 with bigger surface area 54 $m^2\ g^{-1}$ than the CeO_2 8.9 $m^2\ g^{-1}$ presented the complete deposition even at high pH. Thus, we speculate that the surface area of support has an obvious influence on the adsorbing capacity. Nevertheless, Au particles could not completely deposit at pH 9 for the sample Au/SiO_2, as the SiO_2 possessed big surface area around 179 $m^2\ g^{-1}$. This means that the colloid solution also impacts the amount of Au deposition. Therefore, the Au particles distribution and the loading content are jointly dependent on the colloid solution pH and the surface area of support with the former as major factor. These two factors may also explain the different adsorption rate of the colloids with changing support.[8] The support with high isoelectric point and big surface area presents high adsorption rate of the Au particles.

Combing with the relationship between colloid solution and isoelectric point of support, we deduce that the dependence on colloid solution pH and isoelectric point may be due to the nature of the protecting agent used with its negative charges, as shown in Figure. 4. The negative charges of PVA may shield the charges of the support and the gold clusters under the conditions of the colloid solution pH much above isoelectric point of support. During the deposition process, the size of Au particles would grow and part of Au particles could not deposit on the support due to the conflict between the negative PVA and the negative support and Au particles. When the colloid solution pH was approximate the isoelectric point of corresponding support, the strong interaction between negative PVA and positive support immediately take place leading to the quickly complete adsorption of Au colloid. When the pH is lower such as around 1, the protective agent PVA could be broken resulting in the grown up of the Au particles. Thus the colloid solution pH value should be adjusted to below the isoelectric point of support and above the 1 to obtain the best Au particles distribution.

The different mean size of Au particles supported on CeO_2 and ZrO_2 were prepared. As we all know, the size of Au particles has a great important role on the activity for many reactions.[11] To investigate this role on oxidative esterification of methacrolein, the catalytic performances of these Au catalysts were tested and the results are shown in Table S1. The catalyst possessing similar size of Au particles provided close catalytic performance indicating that other factors could be excluded. For both Au/CeO_2 and Au/ZrO_2 catalysts, the catalyst with smaller Au particles

10.1002/cctc.201601688

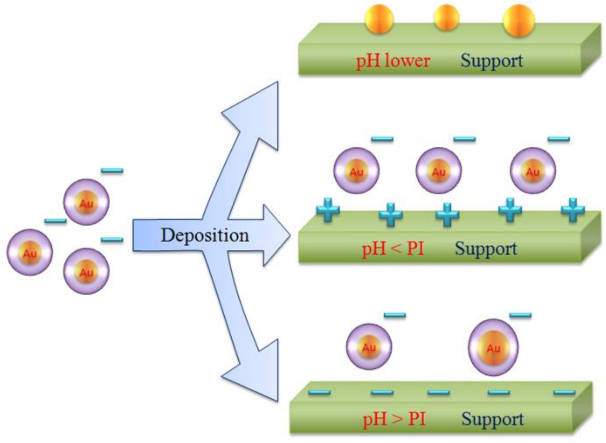

Figure 4. The possible deposition process at different colloid solution pH

presented higher MAL conversion and selectivity for MMA, which could be obtained at medium colloid solution pH. The catalysts with big Au particles prepared at low or high colloid solution pH showed low activity. Thus, the smaller Au particles presented higher activity, which may be due to that these particles could activated the O_2 resulting in the high conversion of MAL and selectivity to MMA.[11b, 12]

Further, the method was applied on other supports by adjusting the pH of colloid solution according the isoelectric point of corresponding support to obtain the similar Au distribution and Au loading and the results were shown in Table 2. The Au loading of all the catalysts were all around 1%, close to the theoretical value 1% according the results of ICP. Only the sample Au/CeO_2 presented much lower Au content than target value, which might be due to the small surface area and the polyhedral structure of the support CeO_2. The TEM technology was employed to determine the distribution of Au particles. As one can see from Fig. 5, Au particles were well dispersed and the mean size was almost identical for the catalysts with the mean size slight bigger than the size of gold colloid. As summarized in Table 2, the mean size of Au particles for all catalysts was similar around 4.4 nm except the Au particles supported on TiO_2 with a slightly bigger mean size around 4.6 nm. These indicated that well distributed Au particles with similar size on different supports were successfully prepared by the simple adjustment of colloid solution pH. Thus, the effect of the size of Au particles on the difference in activities of catalysts could be neglected. The property of support might be responsible to the different activity of catalysts.

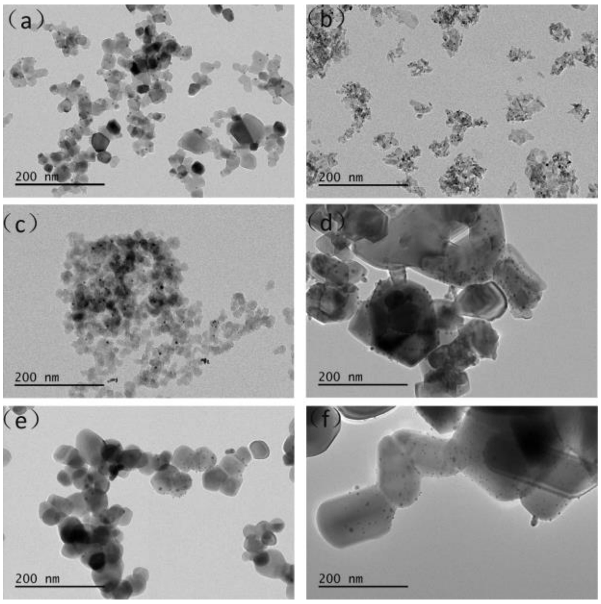

Figure 5. TEM images and size distribution histogram of Au nanoparticles loaded on different supports. (a) Au/TiO_2, (b) Au/Al_2O_3, (c) Au/SiO_2, (d) Au/CeO_2 (e) Au/ZrO_2, and (f) Au/ZnO.

Effects of support on the Au supported catalysts for oxidative esterification of methacrolein

The Au catalysts loaded on different supports were tested for the oxidative esterification of MAL with methanol in the absence of base and the results are shown in Figure 6. All samples presented good activities with the conversion all above 69% especially for Au/Al_2O_3 and Au/ZnO with the conversion 99.6% and 99.9%. However, the Au nanoparticles supported on TiO_2 and SiO_2 showed low selectivity for MMA and acetal, which were both produced by hemiacetal as important intermediate. The Au particles loaded on CeO_2 and ZrO_2 had a low selectivity of MMA with a higher selectivity of acetal and the selectivity of other by-products was blow 7%. Au/Al_2O_3 and Au/ZnO also presented higher selectivity of MMA and lower selectivity of acetal than other catalyst. Among of all the catalysts, the sample Au nanoparticles supported on ZnO possessed the best performance with the yield of MMA 85.9%.

Table 2. Properties of Au catalysts loaded on different supports

Catalyst	Au loading[a] [%]	Au particle size[b] [nm]	PH value	Surface area[c] [m^2g^{-1}]	Au $4f_{/2}$[d]
Au/TiO_2	1.08	4. 6 (5.4)[e]	5	55	83.3
Au/SiO_2	1.17	4.5 (6.7)	3	**183**	84.0
Au/Al_2O_3	1.04	4.2 (5.6)	8	154	84.0
Au/CeO_2	0.86	4.4 (5.8)	3	8	84.0
Au/ZrO_2	0.97	4.5 (5.8)	5	18	83.8
Au/ZnO	1.14	4.4 (5.1)	8	4	83.3

[a] Calculated from ICP-OES data. [b] Evaluated from TEM. [c] Determined by N2-BET. [d] Obtained by XPS data.[e] The value in parentheses is Au particle size of catalysts after reaction.

10.1002/cctc.201601688

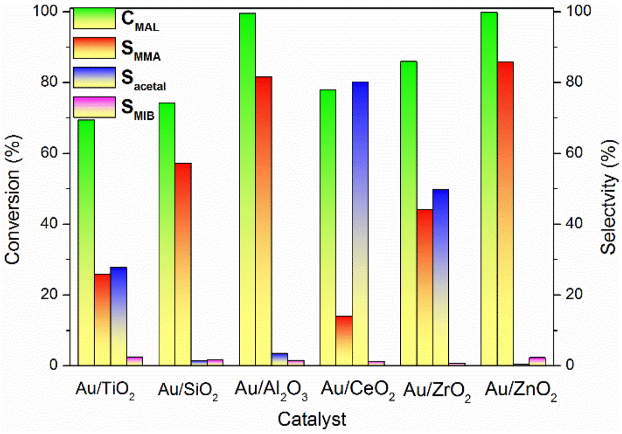

Figure 6. Catalytic performances of Au catalysts loaded on different supports. Reaction conditions: catalyst, 0.50 g; CH_3OH/MAL = 30:1 (molar ratio); CH_3OH, 15 mL; P (O_2) = 0.2 MPa; T = 343 K; t = 2 h

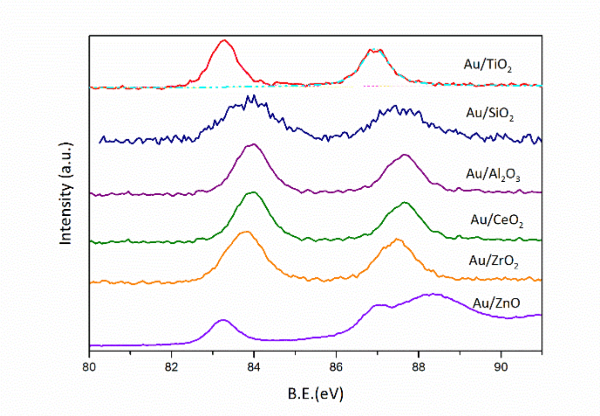

Figure 7. XPS spectra of Au 4f in catalysts with different supports.

Generally, the surface area is also an important factor which could affect the diffusion of the substrates leading to the variation of reaction rate and the BET surface areas of catalysts are presented in Table 2. The sample Au/SiO_2 presented the biggest surface area, but its activity is very low with the yield of MMA 43%. On the contrary, the catalyst Au/ZnO possessed the best performance with the smallest surface area. Obviously, the surface area of the catalyst mainly determined by the support is not the determinant factor affecting the catalytic activity. Other properties of the support need to be investigated.

The chemical adsorption method can be used to determine the strength and amount of acidity, basicity and reducibility for solid catalysts. NH_3-TPD, CO_2-TPD and H_2-TPR were used to analyze the Au catalysts, since it is reported that strong acidity, basicity and reducibility of support are beneficial to the oxidative esterification of aldehyde.[5-6, 13] The NH_3-TPD, CO_2-TPD and H_2-TPR profiles for catalysts loaded on different supports are shown in Figure. S3. The Au/SiO_2 presented the largerst amount of acidic sites, while the Al_2O_3 and ZnO showed nearly no acidity. The sample Au/ZnO presented the largest amounts of basic sites and the Au/Al_2O_3 showed second most amount of basic sites. For all the catalysts, no obvious peak of H_2 reduction below 500 °C was observed. This means Au particles reduction by $NaBH_4$ presented no adsorbed oxygen, which is different from the Au particles prepared by deposition-precipitation (DP) method. Obviously, no correlation between the activity of catalyst and the acidity or reducibility of support could be observed, since the Au/ZnO with the highest activity possessed low acidity and reducibility. ZnO and Al_2O_3 supported Au catalysts were the most efficient catalysts for the oxidative esterification of MAL to MMA, while the use of SiO_2 or TiO_2 as the support provided much poorer catalytic performances. Meantime, the Au/ZnO and Au/Al_2O_3 possessed high densities of basic sites and the SiO_2 or TiO_2 as the support showed low basic sites (Table S2). The trend of basic sites correlates well with that for the change of catalytic performance with different supports (Figure 6). These results allow us to propose that the densities of basic sites of the support may facilitate the oxidative esterification transformation.

On the other hand, the support ZnO and Al_2O_3 bearing the highest isoelectric point around 9 (Table S2) also presented the best activity. The trend of the isoelectric point of the support also is well associated with the variation of catalytic performance. This interesting phenomenon is not reported before. However, the differences between the supports with respect to the activity of the catalysts can presently not be explained by the isoelectric point, and this effect is under research. We preliminarily speculate that the isoelectric point of the support may change the pH of the reaction solution leading to the variation of the activity.

The surface valence state of gold on different supports was analyzed by the XPS technology and the results are shown in Fig. 7. As we can see, all the catalysts showed the spectra with two distinct peaks around 83.9 eV and 87.6 eV for Au $4f_{7/2}$ and Au $4f_{5/2}$ lines, respectively, which are assigned to the Au 4f binding energies of metallic Au.[14] The binding energy of Au 4f for all catalysts differed a little and the binding energies of Au $4f_{7/2}$ of different catalysts are shown in Table 2. The binding energy of Au $4f_{7/2}$ loaded on SiO_2, Al_2O_3 and CeO_2 located at 83.9 eV, which is similar to the bulk Au at 84.0 eV. A slight shift to low binding energies of Au $4f_{7/2}$ for the sample Au/ZrO_2 could be observed. Simultaneously, it is noteworthy that a negative shift toward a lower binding energy region of 83.4 of the Au $4f_{7/2}$ for Au/TiO_2 and Au/ZnO is observed. This means that there is a strong interaction between gold particles and TiO_2 or ZnO and efficient electron transfer from the conduction band of TiO_2 or ZnO to the gold particles.[15]

Nevertheless, the effect of this strong interaction with respect to the shape of Au particles is different and the HRTEM images of these catalysts are shown in Figure 8. The Au particles supported on SiO_2, Al_2O_3, CeO_2 and ZrO_2 are almost spherical and are the same with the native ones. However, the immobilization on the TiO_2 and ZnO does seem to change the shape of these Au particles in this study. The particles clearly appear to be sunk and faceted under the surface if adsorbed on the TiO_2 and ZnO. This anchoring effect to Au clusters is benefit to the stability of the clusters. As shown in Table 2, the size of Au particles supported on TiO_2 and ZnO after reaction increased

10.1002/cctc.201601688

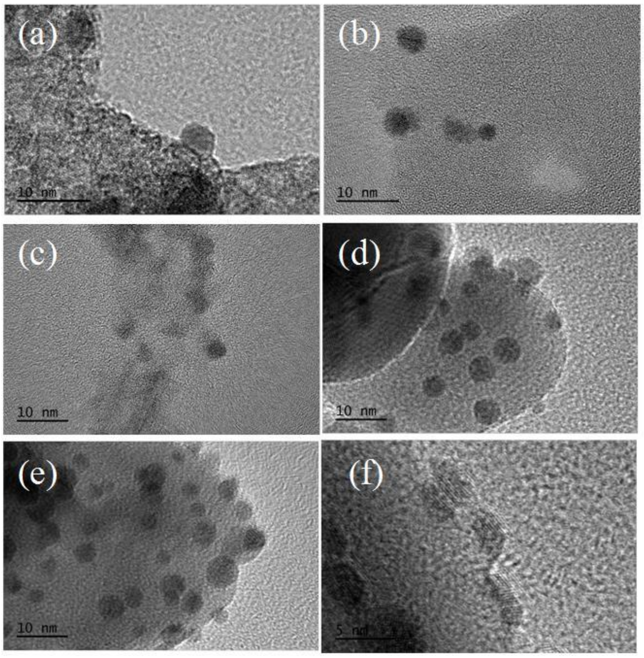

Figure 8. HRTEM images and size distribution histogram of Au nanoparticles loaded on different supports. (a) TiO_2, (b) Al_2O_3, (c) SiO_2, (d) CeO_2, (e) ZrO_2, and (f) ZnO

smaller than other catalysts, indicating that the catalysts Au/TiO_2 and Au/ZnO shown better stability. No leaching of Au after reaction for these two catalysts also confirmed this. On the other hand, the change of geometries could generate the formation of defect on the gold clusters, leading to a change in the number of active corner, edge atoms and the perimeter atoms as previously reported.[16] In our study, the Au particles supported on TiO_2 and ZnO resembled to cuboctahedral and cubo-octahedron truncated morphology respectively. The latter structure presented more amounts of active perimeter and step sites.[17] The Au particles supported on ZnO presented more flat than on TiO_2, indicating the stronger interaction between Au and ZnO.[18] Moreover, combined with the results of XPS and the change of geometries, the interaction between Au and TiO_2 or ZnO could be assigned to the reductive strong metal−support interactions (SMSI) as reported in the literature[15a] and these negative charge Au particles may be benefit to the hydrogenation. That may be why the content of byproduct MIB increased catalyzed by Au/TiO_2 and Au/ZnO than other catalysts prepared by deposition-precipitation method, which the valence state of Au mainly presented part of oxidation state.

The reaction mechanism for the oxidative esterification of aldehydes with alcohols over Au-based catalysts has been investigated recently,[5, 12-13, 19] and two steps are involved in the mechanism. Initially, hemiacetal is formed by condensation reaction between aldehyde and alcohol. Then, the ester is produced by the elimination of H from hemiacetal. During these two steps, the atomic oxygen and the basicity of support play key roles in the oxidative esterification. In our case, the significance of the basicity of support demonstrated obviously, which could enhance the formation of intermediate hemiacetal leading to the improvement of activity. That may be one reason that the Au/ZnO presented the best activity. On the other hand, the active oxygen species could not be observed by H_2-TPR technology, which may be due to that our Au catalysts were prepared by colloid deposition method. Compared with the Au particles prepared by traditional DP method, our Au particles reduced by $NaBH_4$ presented totally metallic state as confirmed by XPS spectra, even for the Au particles supported on TiO_2, ZrO_2 and ZnO negatively charged. The charging of Au particles has less pronounced effect on the activation for O_2 adsorption and dissociation than the size and shape effects, when the Au size goes beyond about 40 atoms (about 1 nm).[20] This charge transformation indicates there is strong interaction between Au and TiO_2 or ZnO, which enhanced the stability and changed the geometries of Au particles particular for the ZnO. The cubo-octahedron truncated morphology for Au/ZnO owned more perimeter sites, which may activated the methoxy species[21] and promote the active oxygen through oxygen spillover.[22] In summary, the Au/ZnO exhibited the best performance due to the strong basic surface sites and the strong interaction between Au and ZnO leading to the anchoring effect and the change of geometries of Au particles which could enhance the stability of catalysts and promote the oxygen mobility and activate the methanol respectively.

There are many important factors that affect the catalytic performance. However, it is unclear that which factor is the determining factor. It is necessary and significant to study the reaction mechanism. Although Xu et al[19] reported the possible reaction process on vapour-phase gold-surface-mediated coupling of aldehydes with methanol, the reaction mechanism in gas-liquid-solid phase particularly under actual reaction conditions is unknown. These factors studied in our paper is the foundation of research for the reaction mechanism. In addition, more technologies in situ are needed.

Conclusions

We prepared Au catalysts by colloid deposition method using PVA as protective agent for the oxidative esterification of MAL to MMA in the absence of base. Three different pre-treatment: thermal treatment, hot water washing and water reflux were compared to remove the PVA stabilizer and no obvious increase of the Au particles were observed after treated by these three methods. The catalyst heated treatment at 300 ºC presented the best activity due to the minimum content of PVA confirmed by DTA and XPS analysis. The heat treatment below 300 ºC or other two methods could not efficiently remove the PVA and the residual PVA decreased the catalytic performance. On the other hand, we found that the colloid solution pH strongly influenced the distribution and loading content of Au particles. The catalyst prepared at proper colloid solution pH around isoelectric point of corresponding support possessed small Au particles and high content Au leading to a high catalytic performance. The effects of the support were also investigated and it is found that the Au/ZnO presented the best activity with the conversion of MAL 99.9% and the selectivity to MMA 85.9% followed by Au/Al_2O_3 and the Au/TiO_2 and Au/CeO_2 had the far less catalytic performance. The best performance may be due to the strong basic surface sites that improved the formation of the intermediate and the strong interaction between Au and ZnO. This interaction caused the anchoring effect and the change of geometries of Au particles which could enhance the stability of catalysts and promote the oxygen mobility and activate the methanol respectively.

Experimental Section

Catalyst preparation

The sol-immobilization method used here has been extensively described elsewhere with slight modification.[23] The colloidal gold solutions were prepared using PVA (Degree of Polymerization: 1700, 88% alcoholysis from Aladdin) as stabilizing ligands and $NaBH_4$ (Sinopharm Chemicals) as reductant. In a typical preparation, a required (PVA/Au (wt/wt) = 1.2) the protecting agent PVA solution (1 wt%) was added to a 1 mmol L^{-1} aqueous gold solution (as $HAuCl_4$ Sinopharm Chemicals, 99.99%) at room temperature under vigorous stirring. The obtained solution was then left under stirring for 5 min. A freshly prepared aqueous solution of $NaBH_4$ (0.1 M, $NaBH_4$/Au (mol/mol) = 5) was then added to form a dark orange-brown gold sol. After 30 min of sol generation, the colloid gold solution was immobilized by adding the support under vigorous stirring. The amount of support material required was calculated so as to have a total final metal loading of 1 wt%. It is noteworthy that the pH of colloid solution needs to be adjusted to the value below the isoelectric point of the support using the 0.1 mol L^{-1} HCl solution. After 1 h, the slurry was collected by vacuum filtration and the catalyst was washed thoroughly with 2L of doubly distilled water to remove all the dissolved species. Finally, the solids were dried under a vacuum condition at 80 ºC overnight. All supports (TiO_2 P25 from Degussa, SiO_2 from Aldrich , γ-Al_2O_3、CeO_2、ZrO_2 and from Aladdin) were pre-treated at 400 ºC before used.

To remove the PVA agent, three different ways were employed as reported: The calcined catalysts were pre-treated at 100-300 ºC under static air for 4 h using a heating rate 5 ºC/min;[24] For the hot water washing, the catalysts was washed with 90 ºC hot water at the final step and then dried at 80 ºC overnight;[9b] For the reflux method, the prepared catalyst was added into the round bottom flask connected to a reflux condenser and placed in an water bath at 90 ºC, under vigorous stirring; The solution was left to reflux for 2 h and then the solids were dried under a vacuum condition at 80 ºC overnight.[9a].

Catalyst characterization

Nitrogen adsorption/desorption isotherms at 77 K were measured using Micromeritics ASAP 2460. Prior to the measurement, all samples were degassed for 4 h at 573 K. The specific surface area, S_{BET} was calculated using BET equation. Transmission electron microscopy (TEM) was performed using JEOL TEM 2011 operated at 200 kV. Samples were deposited on the TEM grids after ultrasonic dispersion in ethanol. The Au loading was determined by inductive couple plasma optical emission spectrometer (ICP-OES) by IRIS Intrepid II XSP (Thermofisher, USA). X-ray photoelectron spectroscopy (XPS) studies were conducted on a PHI5700 spectrometer applying a monochromated Al Kα source. The binding energy scale was corrected for surface charging by considering the C1s peak of contaminant carbon as a reference at 285.0 eV.

Hydrogen temperature programmed reduction (H_2-TPR) was conducted on Autochem II 2920 (Micromeritics, USA). A total of 50 mg catalyst was filled in a quartz reactor and pretreated under Ar flow (20 mL/min) at 120 ºC for 2 h. After the sample cooled to 50 ºC, the powder was performed with a 10% H_2/Ar gas mixture (20 mL/min) from 50 to 850 °C (20 °C /min). The consumption of hydrogen was monitored online using a thermal conductivity detector. The temperature-programmed desorption of ammonia and carbon dioxide (NH_3- and CO_2-TPD) experiments were also carried out on Autochem II 2920 (Micromeritics, USA). The samples were pretreated under He flow (20 mL/min) at 120 °C for 1 h. The sample was cooled to 50 °C, and then exposed to 10% NH_3/He mixture or 10% CO_2/He mixture flow (20 mL/min) for 1 h. Then, the sample was flushed under Ar flow at 50 °C to remove physically adsorbed CO_2 or NH_3 until the baseline is horizontal. A CO_2-TPD (or NH_3-TPD) profile of the sample was recorded by increasing the temperature from 50 °C to 700 °C at a heating rate of 10 °C/min under 20 mL/min of Ar flow. The effluent was monitored online by a thermal conductivity detector.

Catalytic reaction

The oxidative esterification of MAL with methanol to MMA was performed in a 50 mL steel autoclave. In a typical experiment, the substrate (25 mmol) and methanol (20 mL) were added into the reactor pre-charged with 0.50 g catalyst. After O_2 charged with 0.3 MPa pressure, the mixture was heated to 80 ºC, and then the catalytic reaction was started by vigorous stirring (800 rpm). After 2 h, the stirring and introducing oxygen were immediately stopped. Sequentially, the reactor was quickly cooled down to room temperature. Next, the excess oxygen was depressurized slowly. The products were analyzed using a gas chromatograph equipped with an FID detector and a capillary column (DB-624, 30 m × 0.32 mm × 0.25 μm) using ethanol as an internal standard for quantification.

Acknowledgements

This work was supported by the National Basic Research Program of China (2015CB251401), the "Strategic Priority Research Program" of the Chinese Academy of Sciences (XDA07070600), the National Instrumentation Grant Program (2011YQ12003907) and Special Funds of the National Natural Science Foundation of China (21127011).

Keywords: supported Au catalysts • oxidative esterification • methyl methacrylate • PVA protecting agent • colloid deposition

[1] K. Nagai, *Applied Catalysis A: General* **2001**, *221*, 367-377.

[2] W. W. Cooper, H. Hemphill, Z. Huang, S. Li, V. Lelas, D. W. Sullivan, *European Journal of Operational Research* **1997**, *96*, 1-35.

[3] J. Han, S. Zhang, J. Zhang, R. Yan, *Rsc Advances* **2014**, *4*, 58769-58772.

[4] K. Suzuki, T. Yamaguchi, K. Matsushita, C. Iitsuka, J. Miura, T. Akaogi, H. Ishida, *Acs Catalysis* **2013**, *3*, 1845-1849.

[5] X. Wan, W. Deng, Q. Zhang, Y. Wang, *Catalysis Today* **2014**, *233*, 147-154.

[6] F.-Z. Su, J. Ni, H. Sun, Y. Cao, H.-Y. He, K.-N. Fan, *Chemistry-a European Journal* **2008**, *14*, 7131-7135.

[7] M. Haruta, *CATTECH* **2002**, *6*, 102-115.

[8] M. Comotti, W.-C. Li, B. Spliethoff, F. Schüth, *Journal of the American Chemical Society* **2006**, *128*, 917-924.

[9] a) J. A. Lopez-Sanchez, N. Dimitratos, C. Hammond, G. L. Brett, L. Kesavan, S. White, P. Miedziak, R. Tiruvalam, R. L. Jenkins, A. F. Carley, D. Knight, C. J. Kiely, G. J. Hutchings, *Nat Chem* **2011**, *3*, 551-556; b) X.

Wang, B. Meng, X. Tan, X. Zhang, S. Zhuang, L. Liu, *Industrial & Engineering Chemistry Research* **2014**, *53*, 5636-5645.

[10] Y.-H. Ke, X.-X. Qin, C.-L. Liu, R.-Z. Yang, W.-S. Dong, *Catalysis Science & Technology* **2014**, *4*, 3141.

[11] a) M. Valden, X. Lai, D. W. Goodman, *Science* **1998**, *281*, 1647-1650; b) F. Pinna, A. Olivo, V. Trevisan, F. Menegazzo, M. Signoretto, M. Manzoli, F. Boccuzzi, *Catalysis Today* **2013**, *203*, 196-201.

[12] B. Xu, X. Liu, J. Haubrich, C. M. Friend, *Nature Chemistry* **2010**, *2*, 61-65.

[13] a) Y. Li, L. Wang, R. Yan, J. Han, S. Zhang, *Catalysis Science & Technology* **2015**; b) Y. Li, L. Wang, R. Yan, J. Han, S. Zhang, *Catalysis Science & Technology* **2016**, *6*, 5453-5463.

[14] E. D. Park, J. S. Lee, *Journal of Catalysis* **1999**, *186*, 1-11.

[15] a) X. Liu, M.-H. Liu, Y.-C. Luo, C.-Y. Mou, S. D. Lin, H. Cheng, J.-M. Chen, J.-F. Lee, T.-S. Lin, *Journal of the American Chemical Society* **2012**, *134*, 10251-10258; b) F. Wang, Y. Jiang, A. Gautam, Y. Li, R. Amal, *ACS Catalysis* **2014**, *4*, 1451-1457; c) J. Zhang, X. Liu, S. Wu, B. Cao, S. Zheng, *Sensors and Actuators B: Chemical* **2012**, *169*, 61-66.

[16] M. S. Chen, D. W. Goodman, *Catalysis Today* **2006**, *111*, 22-33.

[17] a) M. Mavrikakis, P. Stoltze, J. K. Nørskov, *Catalysis Letters* **2000**, *64*, 101-106; b) M. Cargnello, V. V. T. Doan-Nguyen, T. R. Gordon, R. E. Diaz, E. A. Stach, R. J. Gorte, P. Fornasiero, C. B. Murray, *Science* **2013**, *341*, 771-773.

[18] N. Lopez, J. K. Nørskov, T. V. W. Janssens, A. Carlsson, A. Puig-Molina, B. S. Clausen, J. D. Grunwaldt, *Journal of Catalysis* **2004**, *225*, 86-94.

[19] B. Xu, J. Haubrich, C. G. Freyschlag, R. J. Madix, C. M. Friend, *Chemical Science* **2010**, *1*, 310.

[20] A. Roldan, J. M. Ricart, F. Illas, G. Pacchioni, *Physical chemistry chemical physics : PCCP* **2010**, *12*, 10723-10729.

[21] F. Menegazzo, M. Signoretto, F. Pinna, M. Manzoli, V. Aina, G. Cerrato, F. Boccuzzi, *Journal of Catalysis* **2014**, *309*, 241-247.

[22] M. Manzoli, F. Menegazzo, M. Signoretto, G. Cruciani, F. Pinna, *Journal of Catalysis* **2015**, *330*, 465-473.

[23] a) L. Kesavan, R. Tiruvalam, M. H. Ab Rahim, M. I. bin Saiman, D. I. Enache, R. L. Jenkins, N. Dimitratos, J. A. Lopez-Sanchez, S. H. Taylor, D. W. Knight, C. J. Kiely, G. J. Hutchings, *Science* **2011**, *331*, 195-199; b) J. Pritchard, M. Piccinini, R. Tiruvalam, Q. He, N. Dimitratos, J. A. Lopez-Sanchez, D. J. Morgan, A. F. Carley, J. K. Edwards, C. J. Kiely, G. J. Hutchings, *Catal. Sci. Technol.* **2013**, *3*, 308-317.

[24] a) H. Yin, C. Wang, H. Zhu, S. H. Overbury, S. Sun, S. Dai, *Chemical Communications* **2008**, 4357-4359; b) L. Wen, J.-K. Fu, P.-Y. Gu, B.-X. Yao, Z.-H. Lin, J.-Z. Zhou, *Applied Catalysis B: Environmental* **2008**, *79*, 402-409.

Entry for the Table of Contents (Please choose one layout)

Layout 1:

FULL PAPER

The Au supported on ZnO catalyst prepared by colloid deposition presetned high performance on the oxidative esterification of methacrolein to methyl methacrylate due to the strong interaction between Au and ZnO.

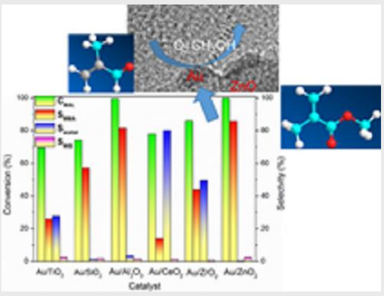

*Yuchao Li, * Yanxia Zheng,] Lei Wang Zhongjun Fu*

Page No. – Page No.

Oxidative esterification of methacrolein to methyl methacrylate over supported gold catalysts prepared by colloid deposition